Title

Physical Exercise Activates Intrinsic CSF Outflow Metrics Detected by Spin-Labeling MRI

Authors

Miyazaki, Mitsue
Malis, Vadim
Yamamoto, Asako
et al.

Publication Date

2022

DOI

10.2139/ssrn.4224903

Magn Reson Med Sci
doi:10.2463/mrms.mp.2023-0005 Published Online: March 11, 2023

MAJOR PAPER

Physical Exercise Alters Egress Pathways for Intrinsic CSF Outflow: An Investigation Performed with Spin-labeling MR Imaging

Mitsue Miyazaki[1*], Vadim Malis[1], Asako Yamamoto[2], Jirach Kungsamutr[3], Linda K. McEvoy[1,4], Marin A. McDonald[1], and Won C Bae[1,5]

Purpose: Cerebrospinal fluid (CSF) clearance is essential for maintaining a healthy brain and cognition by removal of metabolic waste from the central nervous system. Physical exercise has been shown to improve human health; however, the effect of physical exercise on intrinsic CSF outflow in humans remains unexplored. The purpose of this study was to investigate intrinsic CSF outflow pathways and quantitative metrics of healthy individuals with active and sedentary lifestyles. In addition, the effect of exercise was investigated among the sedentary subjects before and after 3 weeks of physical activity.

Methods: This study was performed on 18 healthy adults with informed consent, using a clinical 3-Tesla MRI scanner. We classified participants into two groups based on reported time spent sitting per day (active group: < 7 hours sitting per day and sedentary group: ≥ 7 hours sitting per day). To elucidate the effect of exercise, sedentary individuals increased their activity to 3.5 hours for 3 weeks.

Results: We show that there are two intrinsic CSF egress pathways of the dura mater and lower parasagittal dura (PSD). The adults with an active lifestyle had greater intrinsic CSF outflow metrics than adults with a more sedentary lifestyle. However, after increased physical activity, the sedentary group showed improved CSF outflow metrics. This improvement was particularly notable at the lower PSD, where outflow metrics were highest among the active group.

Conclusion: Our findings describe the relationship between physical activity and intrinsic CSF outflow and show a potential selective outflow pathway with increasing physical activity in the lower PSD pathway, potentially from the perivascular space or cortical venous subpial space.

Keywords: *cerebrospinal fluid, dura mater, intrinsic cerebrospinal fluid outflow pathways, parasagittal dura, spin-labeling magnetic resonance imaging*

Introduction

Alzheimer's disease (AD) is the most prevalent neurodegenerative disorder in the world, currently effecting 50 million people and projected to exceed 152 million by 2050.[1] Here in US, 10% of those aged 65 and older have AD.[2] Neuropathological AD hallmarks are deposition of β-amyloid (Aβ) peptide and hyperphosphorylation of tau, resulting in plaque formation and neurofibrillary tangles.[3] Clearance of waste products from the brain, such as Aβ, was previously thought to occur primarily through blood-brain barrier (BBB) transport.[4] In last decade, the paravascular pathway of metabolic waste clearance, also known as the glymphatic pathway, has been extensively studied.[5–8] These studies, conducted mostly in small animals, have shown that the glymphatic system is responsible for the clearance of Aβ and its waste products to a greater degree than BBB transport.[9]

Due to the role of Aβ clearance in AD, studies of human glymphatic fluid pathways[7,10] have been gaining interest and now stand as one of the most rapidly growing AD research topics today. The concept of glymphatic clearance in the brain was first proposed as a meningeal lymphatic system by which soluble proteins and metabolites are eliminated

[1]Department of Radiology, University of California San Diego, La Jolla, CA, USA
[2]Department of Radiology, Teikyo University, Tokyo, Japan
[3]Department of Bioengineering, University of California San Diego, La Jolla, CA, USA
[4]Herbert Wertheim School of Public Health and Human Longevity Science, University of California San Diego, La Jolla, CA, USA
[5]Department of Radiology, Veterans Affairs Healthcare System, La Jolla, CA, USA
*Corresponding author: Department of Radiology, University of California San Diego, 9472, Health Science Drive, La Jolla, CA 92093, USA. Phone: +1-847-636-7573, E-mail: mimiyazaki@health.ucsd.edu

Received: January 11, 2023 | Accepted: February 3, 2023

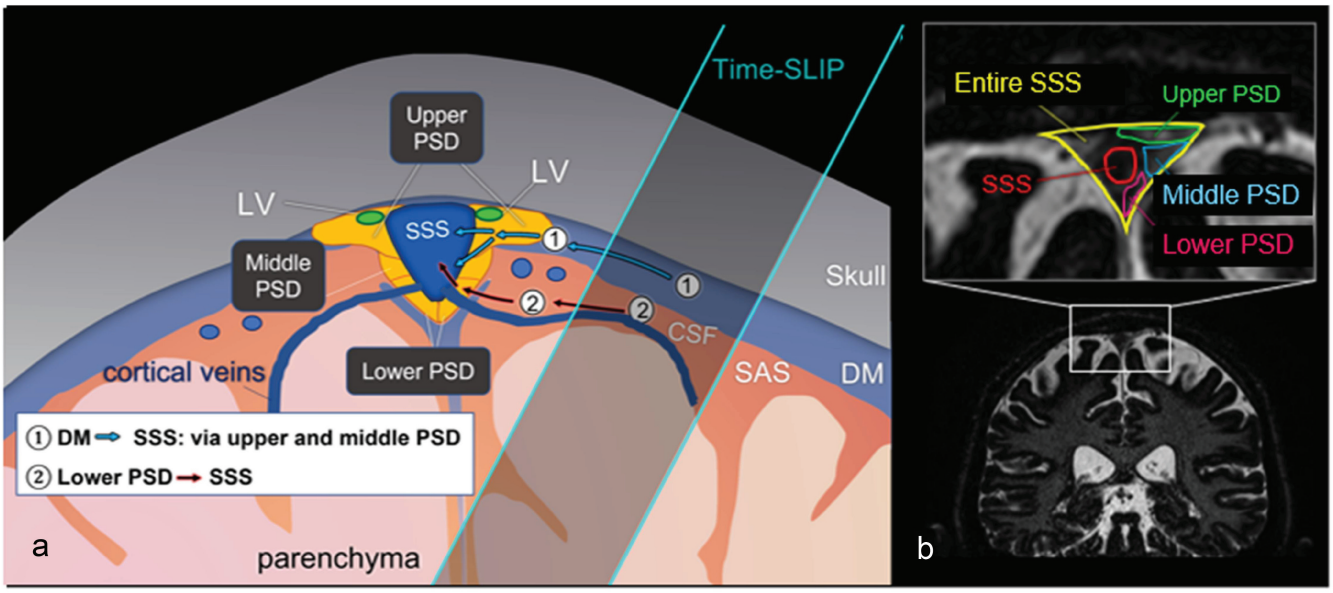

Fig. 1 (**a**) Illustration of potential egress pathways of intrinsic glymphatic fluid. (1) Dura mater pathway: dura mater to upper PSD and/or middle PSD, and then to SSS. (2) Lower PSD pathway: Lower PSD to SSS, potentially via the subpial space or perivascular space of cortical veins. Note that dural lymphatic vessels are observed by Gd-tracer studies which are not visualized by spin-labeling MRI. (**b**) Enlarged coronal T2-weighted image with segmentations showing the entire SSS around the meninges (yellow), upper PSD (green), middle PSD (blue), lower PSD (pink), and SSS (red). DM, dura mater; LV, dual lymphatic vessel; PSD, parasagittal dura; SAS, subarachnoid space; SSS, superior sagittal sinus. (Modified from reference # 17 with permission).

from the central nervous system (CNS) via cerebrospinal fluid (CSF) and interstitial fluid (ISF) exchange, first and most extensively interrogated in animal studies using invasive, ionizing radiation and tracer injection.[6–8,11] In animals, a variety of factors affecting brain waste clearance pathways have also been interrogated, showing an impairment of clearance with aging[12] as well as an improvement with sleep[13] and exercise.[14] Analogous work in humans using both intravenous[15] and intrathecal[16] injections of gadolinium-based contrast agents (GBCA) has revealed the presence of meningeal lymphatic vessels and brain lymphatic clearance via the parasagittal dura (PSD). Using intrathecal administration of GBCA as a tracer, clearance in the human brain has been observed, but over a prolonged period of 48 hours.[16]

We previously introduced a novel MRI method for quantifying CSF outflow in humans that does not require injection of tracers, but instead uses spin-labeling MRI which can detect the perfusion-like movement of endogenously tagged CSF.[17] With this method, we showed net CSF outflow from the dura mater into the superior sagittal sinus (SSS) over a time period of less than 3 seconds. Our prior work detailed multiple potential but distinct anatomic pathways of glymphatic clearance in the brain. After intravenous GBCA administration, meningeal lymphatic vessels in humans and non-human primates have been visualized using MR imaging. In addition, the "classic pathway" of CSF outflow directly from the subarachnoid space (SAS) to SSS via arachnoid granulations has also been proposed, based on anatomy of dissected tissue, but not readily visualized by imaging.[18,19] Utilizing noninvasive, spin-labeled tagging of CSF, our prior work has identified anatomically distinct CSF egress pathway of the dura mater to the SSS via PSD, as shown in Fig. 1.[17] In addition, we also observed that CSF outflow metrics at the upper PSD and SSS regions were significantly lower in older adults compared to a younger cohort, potentially consistent with known effects of age on glymphatic clearance.[17] However, more work remains to be done to uncover the importance of multiple potential anatomically distinct CSF or glymphatic egress pathways, both in terms of normal physiologic function and selective waste-clearance reserve in the setting of disease.

It has been well established by WHO guideline 2020 that there is a strong association between physical exercise and maintenance of cognitive brain health.[20] Documented positive effects include changes in brain volume and connectivity, cerebral perfusion, and synaptic plasticity, among others. In young and aged mice, voluntary running enhances glymphatic influx in awake.[14,21] Aerobic exercise training has been shown to improve cerebral blood flow not only in young adults,[22,23] but also in sedentary older adults.[23,24] Physiologic forces such as arterial pulsation, vasomotion, and respiration drive the glymphatic fluid flow that is critical to maintain brain homeostasis.[25] A study in aged mice using *in vivo* two-photon imaging showed that voluntary wheel running promotes glymphatic clearance by influx through the paravascular space, ISF exchange, and efflux through ISF drainage.[14] However, the effects of exercise on

glymphatic clearance in humans remain unexplored, primarily because of a lack of adequate imaging methodology to noninvasively characterize this low-pressure fluid transport system in the brain.

The aim of the present study was to investigate intrinsic CSF outflow pathways and their quantitative metrics using our newly developed spin-labeling MRI technique[17] among healthy adults with active lifestyles and those with more sedentary lifestyles. We also examined longitudinal changes in intrinsic CSF outflow metrics among sedentary adults after an increased physical activity for 3 weeks. We will use the term CSF or glymphatic fluid interchangeably throughout this manuscript to encompass ISF-CSF fluid.

Materials and Methods

Experimental design

The study was approved by our Institutional Review Board of University of California, San Diego (Approved No. 200335). We obtained a written informed consent from all study participants. The study design was observational: Randomization of participants was not required, and no prior sample size calculation was performed since this was our initial study of its kind.

Participants

We recruited 18 healthy adults from the local community who had no known neurodegenerative disease, pulmonary disease, cardiovascular disease, hypertension, or diabetic disease. Although not measured, we assumed the healthy subjects had a normal range of respiratory rate, HbA1C, and blood pressure. All participants were administered the International Physical Activity Questionnaire (IPAQ-SF).[26] The IPAQ-SF assesses amount and intensity of physical activity and sedentary time during the past week. According to Ding et al.,[25] vigorous is defined by the IPAQ-SF as physical activity that "takes hard physical effort and makes you breathe much harder than normal"; moderate is defined as "activities that take moderate physical effort and make you breathe somewhat harder than normal"; and walking exercise. All participants had resting heart rate between 50 and 75 beat per minute.

We classified participants into two groups based on reported time spent sitting per day: active group: < 7 hours sitting per day with ≥ 5 hours of physical activity per week and sedentary group: ≥ 7 hours sitting per day. WHO recommended 150–300 minutes of moderate physical activity per week.[20] After participating in the baseline imaging session, the sedentary group was asked to increase their activity level by performing any type of physical activity for at least 3.5 hours per week for 3 weeks (see Table 1 for type and amount of activity engaged by each participant). They then participated in a second imaging session. To elucidate intrinsic CSF egress pathways and quantitative metrics, physical activity was continued for 3 weeks.

Table 1 shows the participant demographics and their self-reported physical activity and sedentary time. There were 9 participants in the active group (5 males and 4 females; age range 19–65 years; mean age, 43.9 $\pm$ 17.6 years) and 9 participants in the sedentary group (5 males and 4 females; age range 19–64 years; mean age, 38.8 $\pm$ 12.9 years). Table 1 data reports that subject 2 (62-year-old active male) had over 15 hours per week of physical activity due to his walking, with fitbit counts of 25000 steps per day for 5 days. Another example was subject 16 (19-year-old sedentary male student) who was sitting daily about 12 hours due to studying and taking online courses during the coronavirus disease 2019 (COVID-19) period. Note that most of sedentary individuals did not change their sitting period between before and after 3 weeks of activity due to their workstyles, except subject 10 (48-year-old male) who reduced sitting hours from 7.5 hours to 6 hours after exercise. Subject 12 (30-year-old male) was categorized in the sedentary group due to sitting about 10 hours per day, but his physical exercise was originally 6 hours per week and had increased to 10 hours per week.

MR protocol

All MRI examinations were performed on a clinical 3-T MRI scanner (Vantage Galan; Canon Medical Systems, Tochigi, Japan), equipped with a 32-ch head coil. All scans were acquired at mid-day (between 10 am and 2 pm local time) to control circadian effects. The subjects did not exercise on the day of MRI scan. Thus, the last physical activity was performed at least a day before the MRI study or at least 12 hours between the acquisition time and the last major physical activity. Sequence parameters were similar to the previous report.[17] However, to improve the accuracy of signal increase ratio (SIR) curve fitting, the temporal resolution near inversion time (TI) = 1250 ms was increased since the preliminary scans showed it to be the TI where the peak flow occurs.[17] In a total, we collected 9 temporal points (9 TIs).

(1) T2-weighted 2D fluid attenuated inversion recovery (FLAIR), TR = 10000 ms, effective TE (TE_{eff}) = 92 ms, echo train spacing (ETS) = 11.5 ms, TI = 2800 ms, flip angle/refocusing angle = 90/170º, 1 average, 25 slices, 2 mm thick, matrix = 384 × 364 (768 × 738 after interpolation), FOV = 22 × 22 cm, parallel imaging factor of 2.8, and acquisition time of 3 min 38s.
(2) T2-weighted 3D centric *ky-kz* k-space ordering single-shot fast spin echo (cSSFSE) parameters are TR = 4200 ms, TE_{eff} = 121 ms, ETS = 6.5 ms, number of shots = 1, flip/flop = 90/120º, matrix size = 432 × 432 (864 × 864 after interpolation), FOV = 22 × 22 cm, 80 slices, 0.6 mm thick, near isovoxel resolution of 0.3 mm × 0.3 mm × 0.3 mm after interpolation, parallel imaging factor of 3, and acquisition time of 2 min and 45s.
(3) Ungated 4D CSF spin-labeling MRI parameters with 3D cSSFSE readout are TR = 5400 ms, TE_{eff} = 30 ms,

Table 1 Demographics of the participants with daily sitting period at various exercise levels

Group	Subject ID	Gender	Age (yo)	Height (cm)	Weight (kg)	BMI	Sitting per day (hr)	Activity type	Activity per week (hr)
Active									
	1	M	58	179	74	23	5	V, M, W	5
	2	M	62	168	62	22	5	W	15
	3	M	28	174	67	22	6	V	6
	4	M	19	178	94	30	6	V	5
	5	F	40	164	53	20	6	V	5
	6	F	60	166	63	23	4	W	12
	7	F	36	163	68	26	6	V	5
	8	M	27	174	70	23	5	V	5
	9	F	65	170	58	20	5	V	5
Group average:		5 M , 4F	43.9 ± 17.6	170.7 ± 5.9	67.7 ± 11.7	23.1 ± 3.0	5.3 ± 0.7	-	7.0 ± 3.8

Group	Subject ID	Gender	Age (yo)	Height (cm)	Weight (kg)	BMI	Sitting per day (hr)		Activity type		Activity per week (hr)	
							Pre	Post	Pre	Post	Pre	Post
Sedentary												
	10	M	48	173	74	25	7.5	6	W	W	1.5	10
	11	M	42	173	68	23	9	8	-	M, W	0	8
	12	M	30	176	77	25	10	10	W	V, M, W	6	10
	13	F	64	156	58	24	12	10	-	M, W	0	6
	14	F	28	177	91	29	9	8	-	W	0	4
	15	F	36	168	59	21	12	12	W	V	0.5	3.5
	16	M	19	175	58	19	12	12	V	V, M, W	0.5	3.5
	17	M	42	185	79	23	10	8	M	V, M, W	2	6
	18	F	40	169	58	21	12	12	W	W	0.5	4
Group average:		5 M , 4F	38.8 ± 12.9	172.4 ± 7.9	69.1 ± 11.9	23.1 ± 2.9	10.4 ± 1.7	9.6 ± 2.2	-	-	1.2 ± 1.9	6.1 ± 2.7

Data are presented as mean ± standard deviation. BMI, body mass index; M, moderate – defined as "activities that take moderate physical effort and make you breathe somewhat harder than normal"; V, vigorous – defined by the IPAQ-SF as physical activity that "takes hard physical effort and makes you breathe much harder than normal"; W, walking exercise.

ETS = 5.0 ms, number of shots = 1, flip/refocusing angle = 90/180°, matrix size = 368 × 368 (736 × 736 after interpolation), FOV = 25 × 25 cm, parallel imaging factor of 3, 8 slices, 1 mm thick (0.5 mm after interpolation), tag-on and tag-off acquisition time of about 54 sec. Images were acquired for the TI of 500, 750, 1000, 1150, 1250, 1350, 1500, 2000, and 3000 ms.

Detailed methodology of time-resolved non-contrast MRI has been previously described by Malis et al.[17] We used the simple subtraction of tag-off from the tag-on images to visualize intrinsic CSF moves out from the tagged region. To elucidate quantitative metrics of intrinsic CSF outflow, SIR was calculated using SIR = |Tag-on – Tag-off|/|Tag-off| to observe a perfusion-like function.

Time-resolved non-contrast MRI was acquired and reconstruction of each tag-on and tag-off post-processing was performed. An adiabatic spatially selective inversion recovery pulse, time-spatial labeling inversion pulse (Time-SLIP), was used in the tag-on acquisition. A tag-on and tag-off alternate acquisition and subtraction technique was used with 3D cSSFSE. The detailed tag-on and tag-off 3D acquisitions were also described in the work by Malis et al,[17] as well as the applications in the non-contrast MR angiography and perfusion techniques.[27–30] Of note, we confirmed[17] that the technique measures CSF signal while suppressing blood signal by using a long effective TE of 300 ms, since the T2 of blood is shorter around 60 ms.

Experimental studies

The 3D coronal imaging slab was placed at the top of the head and an oblique tag pulse was applied alongside the SSS. The detailed anatomies of dura mater, PSD, and SSS were visualized using coronal images of T2-weighted FLAIR and T2-weighted 3D cSSFSE with distinct intrinsic contrast. Our ungated 4D CSF spin-labeling MRI technique was optimized to acquire TI of 500, 750, 1000, 1150, 1250, 1350, 1500, 2000, and 3000 ms, a total of 9 acquisitions (each TI with a scan time of 54 sec.) to have higher temporal resolution near TI = 1250 ms, where a peak height (PH) was observed. Higher temporal resolution was utilized to improve our SIR curve fitting. In addition, due to the complex structure of the meninges, we sought to minimize the physiological effects of respiration, cardiac pulsation, etc., by using the ungated method with a long TR. We have studied both simple subtraction of tag-on and tag-off images as well as the SIR fitting at each TI period, after registration of both images.

Data analysis and post-processing

To differentiate the dura mater pathway and the lower PSD pathway, we segmented the PSD to upper, middle, and lower PSD, SSS, and entire SSS, as shown in Fig. 1. We investigated the effect of exercise on intrinsic CSF outflow metrics in these segmented areas to identify potential distinct egress pathways. Regions were manually selected for each participant on the tag-on image (TI = 500 ms) away from the tagged region by an MR physicist and a medical doctor together. We carefully selected the 5 ROIs from images of TI of 500 ms together with T2-weighted FLAIR and T2-weighted 3D cSSFSE because the image contrast of TI of 500 ms provides well-defined regions of PSD in bright signal with dark SSS signal. For both volumes (tag-on and tag-off), voxels with intensity values outside the range (mean $\pm$ 2 standard deviation [SD]) were excluded from further analysis. This method was applied to avoid contamination of any pulsatile blood signal in the voxels. This ensures that our tagged MRI signal is from the CSF and not the blood.

Normal distribution of intensities in tag-on and tag-off images is expected and the range of (mean $\pm$ 2 SD) contains 95% of the voxels in the selected ROI.[31] To determine the percent SIR from outflow, tag-off images were subtracted from tag-on images, and the absolute value of the difference was then divided by tag-off images, as |tag-off – tag-on|/|tag-off|.

This was performed for each TI, resulting in a time-varying signal increase at each voxel. The ROI averaged values (y) were then used to perform least-squares fit for the TI-dependent gamma variate function.[32] Fitting results produced estimates for five outflow metrics including: PH, time-to-peak (TTP), mean transit time (MTT; width at half the PH), relative CSF volume (rCFV; area under the curve), and relative CSF flow (rCFF; rCFV divided by MTT). We determined how these outflow metrics varied by three groups: active, sedentary pre-exercise, and sedentary post-exercise.

Statistical analysis

Significant differences in CSF flow metrics between different activity groups and ROIs were tested with the Multivariate-ANOVA test, with Bonferroni correction for multiple comparisons. Normality of distribution for all the variables was confirmed by performing the Shapiro-Wilk test. Statistical analyses were performed using IBM SPPS v26 (IBM, Armonk, NY, USA).

Results

Tag-on and tag-off subtraction and SIR

Figure 2 shows tag-off, tag-on, subtraction, and colored SIR images with a position of the tag pulse in the oblique. The subtraction of tag-off from the tag-on enlarged images demonstrated the tagged CSF signal moving out from the tag region to the upper PSD and subpial space following the shape of the brain. To elucidate the relationship between the tagged signals with varying TIs, the time course of tagged CSF signals was observed from the subtraction images.

Figure 3 shows the tag-on and tag-off subtraction color map images of a healthy young active participant (28-year-old male) with regular exercise (6 hours per week), and a healthy young sedentary participant (19-year-old male) at the baseline (pre-exercise) (< 1 hour per week) and after 3 weeks of increased physical activity (post-exercise) (3.5 hours per week). On the active individual, intense signals at upper PSD and lower PSD can be observed between TI of 1150–1500 ms with explicit pathways of the upper PSD, and the lower PSD evident in a time-resolved manner (Fig. 3a). The enlarged image unambiguously shows that the tagged CSF in the upper and lower PSD traveled around the SSS. Note that the sedentary participant at baseline shows less CSF signal from the dura mater and PSD (Fig. 3b), whereas post-exercise images showed clear signals in both PSD and lower PSD, even around the SSS (Fig. 3c). In addition, the second pathway of the lower PSD was also observed in the active and post-exercise participants. Again, we observed the signals indicating both pathways of CSF outflow in a time-resolved

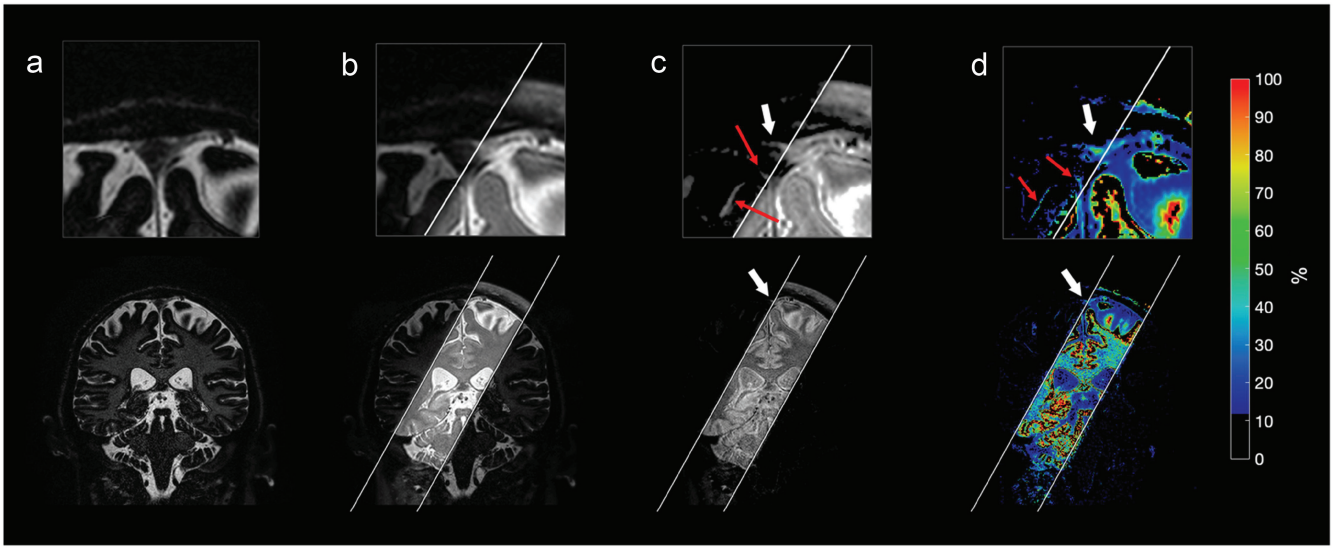

Fig. 2 Coronal spin-labeling (**a**) tag-off, (**b**) tag-on, (**c**) subtraction image of tag-off from tag-on with an absolute value, and (**d**) SIR color map calculated by |tag-off – tag-on|/|tag-off|. White parallel lines show the location of the oblique Time-SLIP tag pulse. Note that CSF signals outside of the tag pulse have moved out from the tagged region and visible at PSD in enlarged images in (**c**) and (**d**), as shown by white arrows. In addition, tagged CSF signals can be seen in the subpial space following the contour of the brain (red arrows). CSF, cerebrospinal fluid; PSD, parasagittal dura; SLIP, spatial labeling inversion pulse; SIR, signal increase ratio.

manner. As an example, indicated by the subtraction color maps in Fig. 3a, we observed the clear signals out from the tagged region to the upper, middle, and lower PSD areas in the active group.

Quantitative CSF outflow metrics

As the simple color maps show that tagged signals have moved from the tag region to PSD and lower PSD, qualitative metrics of CSF outflow were calculated using SIR vs. TI data. Figure 4a shows the SIR images at the entire SSS region at varying TI periods fused with tag-off image at TI of 500 ms in a young sedentary participant before (Fig. 4a top) and after 3 weeks of exercise (Fig. 4a bottom). Figure 4b shows quantitative metrics of PH, TTP, MTT, rCFV (%·s), and rCFF (%). Note that quantitative outflow metrics after exercise greatly increased, as compared to before exercise, in PH (51% to 167%), rCFV (55%·s to 199%·s), and rCFF (54% to 177%). In addition, color maps showed bright signals in the entire SSS region post-exercise (Fig. 4a bottom). Bright white signals at the SSS region indicated high signals. At increasing TIs, this technique captured snapshots of CSF outflow from PSD into SSS, visualized in time-resolved images (Fig. 4a).

Quantitative measures at segmented ROIs

As indicated in Fig. 1b, ROIs were drawn to segment upper PSD near the dura mater, middle PSD and lower PSD, SSS, and entire SSS of meninges. The lateral side of PSD was separated to middle and lower PSD to identify the location of the second pathway. We measured three groups (active, sedentary, and sedentary post-exercise) with 5 ROIs (upper PSD, middle PSD, lower PSD, SSS, and entire SSS of meninges), as shown in Fig. 5a. We tried to separate the lateral side of PSD in a half to middle PSD and the other half to the lower PSD. In all 5 ROI measures, the active group shows the highest signal, followed by the post-exercise sedentary group and pre-exercise sedentary group (Fig. 5b). Note that the pre-exercise sedentary group had the smallest signal in the lower PSD; however, it was substantially improved post-exercise. Figure 5c shows the cluster plots of rCFV, rCFF, and PH vs. age at the five ROIs, clustered by the subject groups of active participants (pink cluster) and sedentary participants before (green cluster) and after (blue cluster) increasing activity levels. Quantitative metrics of PH, rCFV, and rCFF were higher in the sedentary group post-exercise than pre-exercise. More interestingly, in some ROIs (i.e., Upper PSD and SSS), post-exercise increase in outflow metrics in sedentary subjects resulted in a new blue cluster that resembles the red cluster of the active subjects. In addition, in the lower PSD, comparison of green vs. blue (post-exercise) cluster suggested generally greater increase of values in the older subjects. Table 2a shows all quantitative metrics of PH, TTP, MTT, rCFV, and rCFF in 5 ROIs and area in active, sedentary, and post-exercise sedentary groups. Interestingly, comparison of pre-exercise and post exercise in the sedentary group suggested that the PH of middle PSD increased from 138.2% to 267.0% (less than double increase), whereas the PH of lower PSD increased from 44.4% to 171.7% (nearly 4 times increase). The rCFV and rCFF showed similar increases in the lower PSD. The TTP of lower PSD in the active and post-exercise sedentary

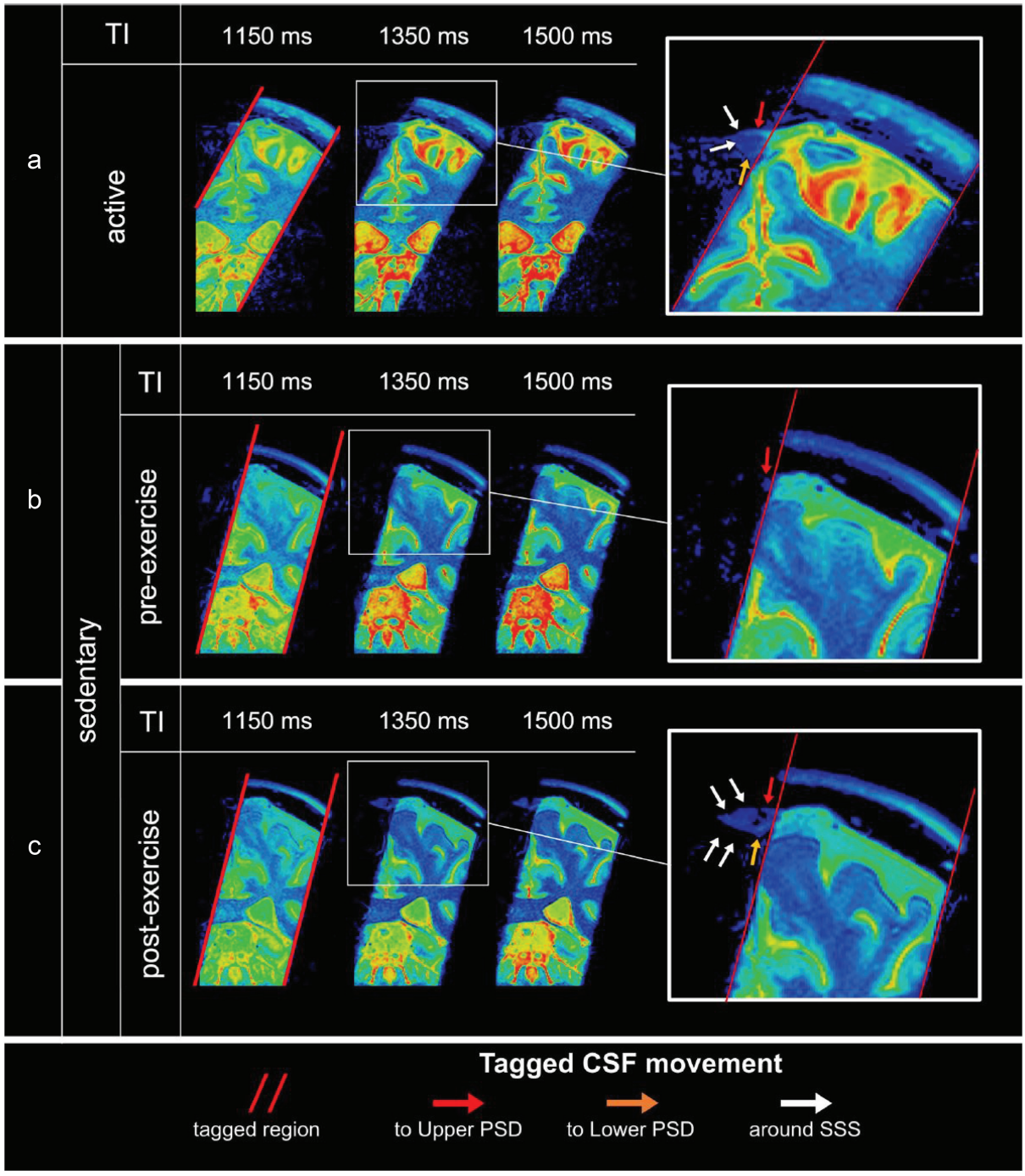

Fig. 3 Simple subtracted images of tag-on and tag-off images of an active lifestyle participant (28-year-old male) (**a**), and a sedentary participant (19-year-old male) before (**b**) and after increase in physical activity for 3 weeks (**c**). Red rectangle boxes show the oblique tag region. Enlarged image of (**a**) at TI of 1350 ms clearly shows tagged CSF moving out from the tagged region (left brain hemisphere) to the upper PSD (red arrow) and to the lower PSD (orange arrow) to the SSS. Note that pronounced CSF outflow signals from the tag pulse can be seen at both upper and lower PSD. In contrast, in the sedentary subject, the enlarged (**b**) image shows relatively decreased signals of tagged CSF at the PSD. The enlarged image (**c**) after exercise clearly shows tagged CSF moving out from the tagged region to the upper PSD (red arrow), the lower PSD (orange arrow), and around the SSS (white arrows), and to the lower PSD, similarly to the active participant. Note that in the post-exercise image, prominent CSF signals flowing out from the tag pulse are seen at both the upper and lower PSD, as compared to only within the upper PSD pre-exercise. CSF, cerebrospinal fluid; PSD, parasagittal dura; SSS, superior sagittal sinus; TI, inversion time.

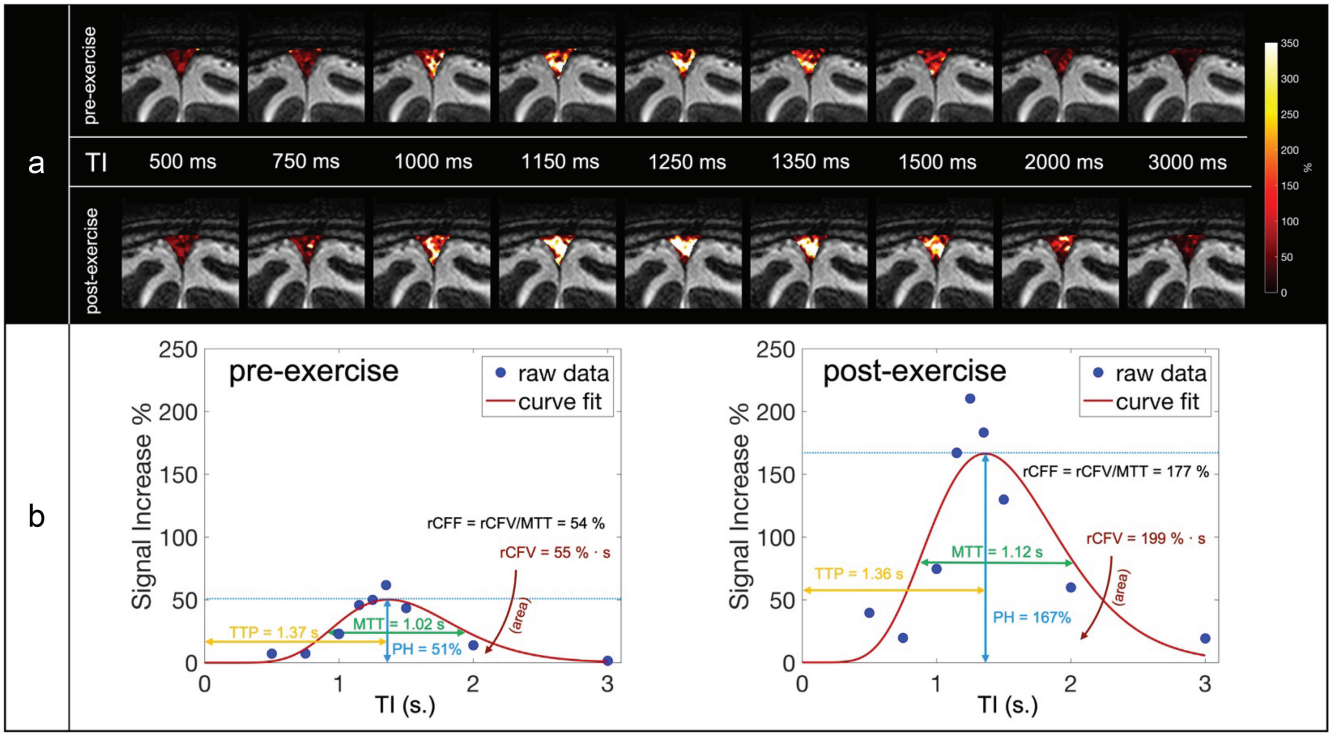

Fig. 4 (**a**) Fusion images of SIR over tag-off image before and after exercise. Note that higher SIR values are seen post-exercise. (**b**) SIR plots of actual measured data (blue) and curve fitting (orange). Circles (blue) show the measured data points, and the orange line indicates the curve fit. Quantitative measures of (Left) before and (Right) after exercise: PH increases from 51% to 167%, rCFV under the curve increases from 55% to 199%·s, and rCFF increases 55% to 177%, which is rCFV divided by MTT, before and after exercise. Note that MTT and TTP are similar, and no notable changes are observed pre- or post- exercise. MTT, mean transition time (s); PH, Peak height (%); rCFF, relative CSF flow (%); rCFV, relative CSF volume (%·s); SIR, signal increase ratio; TTP, time to peak (s).

groups was shortest compared to those of the upper PSD and middle PSD, whereas the TTP of the lower PSD in the sedentary pre-exercise was longest compared to those of upper and middle PSD. The active group showed the highest values in PH, rCFV, and rCFF. All PH, rCFV, and rCFF compared to other groups (posthoc $P < 0.05$). Table 2b shows the average outflow metrics of the five ROIs across all groups.

Discussion

CSF outflow metrics differ between an active lifestyle group and sedentary lifestyle group and can change before and after exercise

We have demonstrated possible CSF outflow pathways of upper PSD from dura mater to SSS and the lower PSD to SSS, as well as their quantitative differences between human subjects with different lifestyles and physical activities. We observed a noticeable difference of CSF outflow metrics between subjects with active vs. sedentary lifestyles, as well as longitudinal changes CSF egress in response to exercise intervention in the sedentary group. Among the different ROIs, the lower PSD showed the smallest PH, rCFV, and rCFF in sedentary participants before they increased their physical activity levels. After 3 weeks of increased activity (> 3.5 hours per week), the sedentary group showed a significant increase in CSF outflow metrics of PH, rCFV, and rCFF in all ROIs, with values approaching that of the active lifestyle group. The greatest improvement of quantitative flow measures following increased activity was observed at the lower PSD. In consideration of circadian effect, as stated in the Materials and Methods, we scanned all subjects between 10 am and 2 pm local time and our subjects had at least 12 hours between our MRI acquisition and the last physical exercise to minimize any circadian rhythm and physiological effects.[33]

Differential effects of exercise on two CSF outflow pathways

Using a simple subtraction of time-resolved images, we observed the movement of the endogenously tagged intrinsic CSF signals from the tagged region of dura mater to upper PSD and another pathway of the lower PSD. Both active and post-exercise sedentary groups unambiguously showed the CSF signal at the dura mater to PSD (pathway 1) and the lower PSD (pathway 2) as demonstrated in Fig. 1. In addition, quantitative metrics of TTP also indicate a faster time to peak in active and post-exercise sedentary groups that reflects a different pathway from the upper PSD, supporting

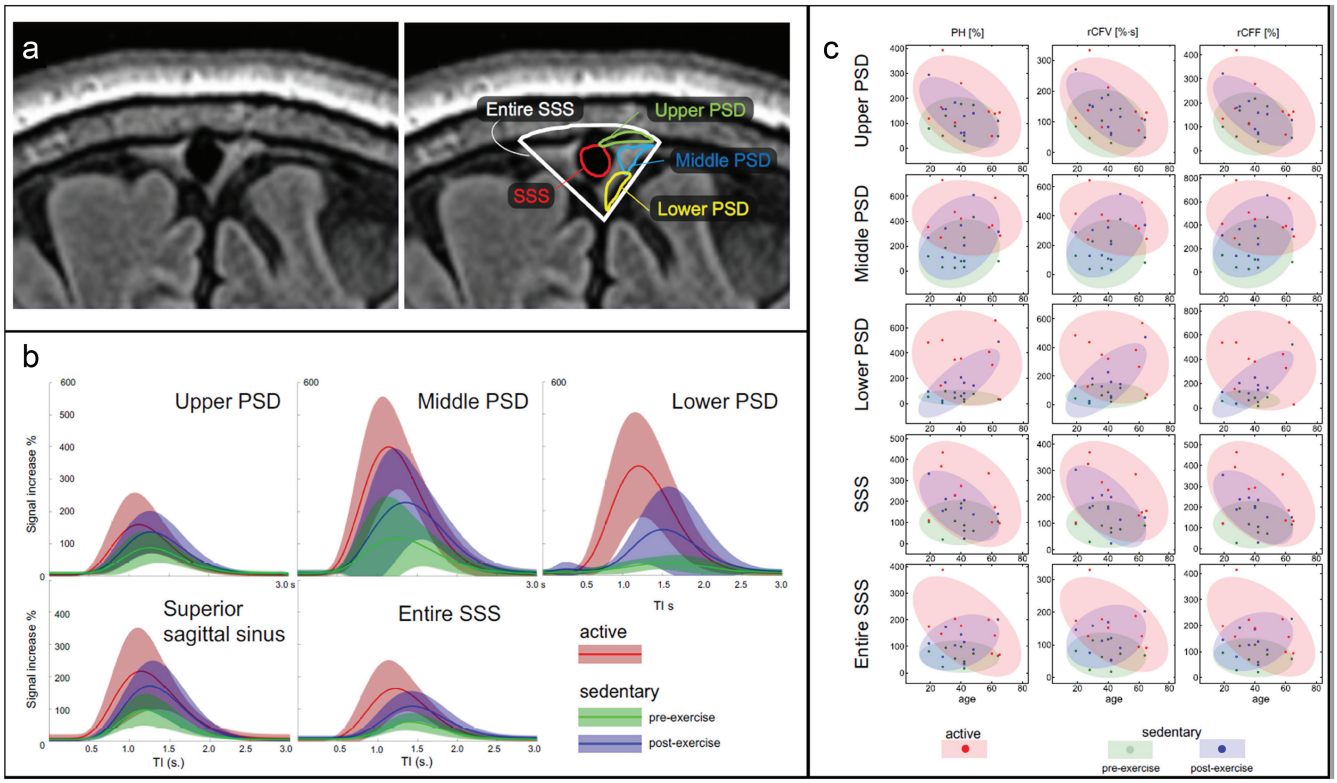

Fig. 5 (**a**) Segmentation of meninges region over the FLAIR image. The PSD was segmented to upper, middle, and lower PSD, SSS, and entire SSS. (**b**) CSF outflow curves of active adults, sedentary adults, and sedentary adults after 3 weeks of physical exercise at the upper PSD, middle PSD, lower PSD, SSS, and entire SSS. Note that the active adults show high quantitative metrics in all regions. The sedentary adults show lower quantitative measures; however, after 3 weeks of increased physical activity, there is substantial improvement in all regions, with incremental increase most pronounced in the lower PSD. (**c**) Plots of the various regions with age for PH, rCFV, and rCFF in active lifestyle adults, sedentary lifestyle adults, and the sedentary adults after 3 weeks of physical exercise (post-exercise). All metrics show increase or improvement of CSF flow among the sedentary adults after physical exercise. Shades indicate a SD range of the curve fits. The sharp oval indicates less SD and circular shape indicates higher SD or more scatted data. The young sedentary cohort demonstrated an increase in the upper PSD, while the older sedentary group showed selective signal increase at the lower PSD. CSF, cerebrospinal fluid; FLAIR, fluid attenuated inversion recovery; PH, peak height; PSD, parasagittal dura; rCFF, relative cerebrospinal fluid flow; rCFV, relative cerebrospinal fluid volume; SD, standard deviation; SSS, superior sagittal sinus.

the lower PSD pathway. The active adult group shows substantially higher signals at both upper PSD and lower PSD, compared to those of the sedentary group before exercise. The pre-exercise sedentary group demonstrated distinctly low PH, rCFV, and rCFF values at the lower PSD. This may imply that there is less CSF outflow from the lower PSD to SSS by pathway 2 among sedentary adults, who instead might maintain the minimally required CSF outflow from the PSD pathway.

In addition to the entire SSS region, all other ROIs (upper PSD, middle PSD, lower PSD, and SSS) showed an increase in CSF outflow metrics post-exercise in the sedentary cohort, with the largest changes observed in the lower PSD among older individuals and in the upper PSD in younger adults. Although our sample size is small, these results may indicate the potential for age-dependent CSF pathway outflow recruitment; specifically that older sedentary adults may recruit the second, subpial space pathway of CSF egress in response to exercise intervention in contrast to younger adults, which demonstrate that overall CSF outflow metric increases by increasing dynamic range at the level of the dura mater pathway.

In our results, tagged CSF signals in the subtraction images and quantitative metrics of CSF with earlier TTP timing support the presence of a second, distinct CSF outflow pathway at the lower PSD. In prior work, Pollock et al. detailed the anatomy of perivascular space (PVS) of the basal ganglia, demonstrating two distinct leptomeningeal membranes in basal arterioles and venioles and a single leptomeningeal membrane in cortical arterioles via electron microscopy.[34] Other work has demonstrated that the PVS between the two leptomeningeal membranes in the basal arterioles and venioles directly communicates with the SAS, whereas the PVS in cortical arterioles and venioles, closer to the location of our tag near the SSS, has a single leptomeningeal membrane which communicates with the

Table 2a Quantitative metrics of 5 ROIs in active, sedentary, and post-exercise sedentary groups

Group	ROI	Area (cm^2)	PH %	TTP (ms.)	MTT (ms.)	rCFV (%· s)	rCFF %
Active							
	Upper PSD	0.116 ± 0.030	168.4 ± 101.2	1176 ± 149	1821 ± 108	146.9 ± 080.2	184.0 ± 105.4
	Middle PSD	0.031 ± 0.017	426.3 ± 150.4	1178 ± 148	1839 ± 070	384.2 ± 127.6	460.0 ± 158.9
	Lower PSD	0.043 ± 0.021	360.3 ± 188.9	1107 ± 339	1035 ± 584	334.3 ± 162.0	390.9 ± 205.1
	SSS	0.030 ± 0.010	235.7 ± 125.1	1248 ± 211	1864 ± 111	220.9 ± 094.9	263.5 ± 126.0
	Entire SSS	0.572 ± 0.190	174.8 ± 093.7	1272 ± 137	1848 ± 066	161.9 ± 072.2	194.9 ± 095.1
	Average	0.159 ± 0.227	273.1 ± 166.6 [A, B]	1196 ± 210 [A, B]	1882 ± 273	249.6 ± 143.4 [A, B]	298.6 ± 176.1 [A, B]
Sedentary							
Pre -exercise							
	Upper PSD	0.138 ± 0.050	191.7 ± 056.0	1296 ± 114	1862 ± 051	095.1 ± 054.9	110.9 ± 065.0
	Middle PSD	0.064 ± 0.023	138.2 ± 137.5	1360 ± 249	1985 ± 278	139.3 ± 116.7	158.1 ± 147.2
	Lower PSD	0.085 ± 0.027	144.4 ± 022.7	1402 ± 169	1105 ± 246	058.9 ± 036.1	053.9 ± 026.4
	SSS	0.055 ± 0.020	199.3 ± 052.7	1220 ± 091	1877 ± 129	096.7 ± 043.8	114.9 ± 056.2
	Entire SSS	0.873 ± 0.283	161.1 ± 029.5	1389 ± 087	1876 ± 050	067.4 ± 034.4	075.9 ± 036.9
	Average	0.243 ± 0.343	191.1 ± 078.6 [B, C]	1327 ± 160 [C]	1925 ± 181	094.7 ± 069.7 [B, C]	107.5 ± 085.6 [B, C]
Post -exercise							
	Upper PSD	0.160 ± 0.046	143.8 ± 070.2	1269 ± 130	1848 ± 046	140.1 ± 060.7	166.1 ± 073.0
	Middle PSD	0.070 ± 0.025	267.0 ± 168.1	1456 ± 224	1896 ± 054	263.3 ± 141.3	300.4 ± 172.2
	Lower PSD	0.094 ± 0.042	171.7 ± 141.4	1225 ± 434	1819 ± 187	174.7 ± 136.8	205.1 ± 142.7
	SSS	0.079 ± 0.036	178.5 ± 083.6	1249 ± 113	1826 ± 032	165.1 ± 077.0	198.7 ± 088.4
	Entire SSS	0.909 ± 0.327	114.9 ± 052.2	1458 ± 141	1916 ± 076	125.0 ± 048.3	138.6 ± 056.2
	Average	0.263 ± 0.358	175.3 ± 118.2 [A, C]	1334 ± 245 [C]	1862 ± 097	173.6 ± 106.8 [A, C]	201.7 ± 122.5 [A, C]

[A]Significantly different than pre-exercise (sedentary) group ($P < 0.05$). [B]Significantly different than post-exercise (sedentary) group ($P < 0.05$). [C]Significantly different than regular exercising group ($P < 0.05$). MTT, mean transit time; PH, peak height; PSD, parasagittal dura; rCFF, relative cerebrospinal fluid flow; rCFV, relative cerebrospinal fluid volume; SSS, superior sagittal sinus; TTP, time-to-peak.

Table 2b Average outflow metrics of 5 ROIs across all groups

ROI	Area (cm^2)	PH%	TTP (ms.)	MTT (ms.)	rCFV %·s	rCFF %
Upper PSD	0.138 ± 0.045	134.6 ± 081.8 [U]	1247 ± 137	844 ± 073	127.4 ± 067.8 [L, U]	153.7 ± 085.8 [U]
Middle PSD	0.055 ± 0.028	277.2 ± 189.4 [P, S, X]	1331 ± 235	907 ± 173	262.3 ± 160.4 [P, S, X]	306.2 ± 198.4 [P, S, X]
Lower PSD	0.074 ± 0.038	219.9 ± 192.4 [X]	1217 ± 354	972 ± 410	213.7 ± 170.3 [P, X]	246.7 ± 203.4 [X]
SSS	0.055 ± 0.031	171.2 ± 105.2 [U]	1239 ± 143	856 ± 099	160.9 ± 088.7 [U]	192.3 ± 110.0 [U]
Entire SSS	0.785 ± 0.304	116.9 ± 077.7 [L, U]	1373 ± 143	880 ± 069	118.1 ± 065.2 [L, U]	136.5 ± 081.4 [L, U]

[L]Significantly different than Lower wall ROI ($P < 0.05$). [U]Significantly different than Upper wall ROI ($P < 0.05$). [P]Significantly different than PSD ROI ($P < 0.05$). [S]Significantly different than SSS ROI ($P < 0.05$). [X]Significantly different than Meninges SSS ROI ($P < 0.05$). MTT, mean transit time; PH, peak height; PSD, parasagittal dura; rCFF, relative cerebrospinal fluid flow; rCFV, relative cerebrospinal fluid volume; SSS, superior sagittal sinus; TTP, time-to-peak.

subpial space.[35,36] Naganawa et al. observed rapid gadolinium-contrast enhancement in the perivascular fluid between the pia sheath and the cortical venous wall, which drains into the inferior aspect of the SSS, using a 3D-real inversion recovery technique,[36] indicating the potential connection between the subpial space and meningeal lymphatics. Our prior and current results also suggest a distinct CSF outflow pathway occurring via the PVS or subpial space at the level of the lower PSD, and that this alternate mechanism may in fact be selectively recruited in older, sedentary adults in the setting of an exercise challenge. Although more work needs to be done, the concept of a recruitable pathway for CSF clearance may offer an exciting prospect for potential new therapeutic approaches in the setting of aging and neurodegeneration.

Effect of exercise on the PVS

In the discussion of the potential mechanistic underpinnings of the observed exercise effects, prior work has demonstrated that aerobic exercise increases cerebral blood flow, oxygen uptake, and glucose utilization in the brain, which may confer benefit for glymphatic outflow by physiologic driving forces.[22] In addition to these potential short-term effects, a component of the durable increased CSF clearance via the upper PSD to the SSS in response to exercise may be mediated by the biological pathways of water channel protein aquaporins (AQPs).[37,38] AQP4 is most abundant in astrocytes in the CNS with the highest expression on perivascular astrocytic end-feet that surround blood vessels. Aaerobic exercise increases cerebral arterial pulsation and enhances rapid transport of water from the extracellular space into the paravascular space via perivascular polarization of AQP4.[39,40] Studies have also shown that the clearance function of the glymphatic system depends on AQP4 in rodent models[41,42] and demonstrate the association between differences in AQP4 expression and localization in human brain samples of AD,[43] subarachnoid hemorrhage,[44] and trauma.[38] Exercise has also been shown to promote the removal of Aβ by AQP4-mediated glymphatic transport in mice.[14,22] Based on AQP4 regulating the water exchange between brain interstitium and glymphatic system, and functional response improvement in AQP4 mediated by cerebral blood active processes,[39] we suggest that the CSF outflow improvement we observed among sedentary adults after increased aerobic exercise could also potentially be mediated by a combination of physiologic driving forces and long-term aquaporin water channel polarization and upregulation, either parallelly or synergistically. Together with the age effect of intrinsic CSF outflow,[17] our studies focus on the egress pathways of intrinsic CSF at the meninges, outside of the brain parenchyma. In the brain parenchyma, an age-dependent decreased diffusivity of the PVS was recently demonstrated using diffusion weighted image analysis along the PVS (DWI-ALPS).[45] Furthermore, another DWI-ALPS study demonstrated a decreased diffusivity in subjects with a mild cognitive impairment or AD.[46] Studying both PVS in brain parenchyma and egress pathways in meninges may offer understanding of the rate limiting regions of CSF-ISF clearance in patients with neurodegenerative diseases.

Other possible outflow pathways

In this study, we are the first to show the effect of exercise on CSF drainage pathways of upper PSD to SSS and the lower PSD to SSS utilizing noninvasive imaging techniques in humans, and to demonstrate a spatially selective, durable increase in CSF egress via the lower PSD. As seen in the subtracted images and SIR images, we postulate a distinct, recruitable pathway corresponding to ISF-to-CSF egress in the subpial space,[36] and other pathways like diploic space[47] and skull base,[48] although ultimately the physiologic significance of the finding remains unclear, and it remains currently unexplored if these glymphatic drainage pathways also exist in humans. It is, nevertheless, tantalizing to postulate that an interplay between short- and long-term exercise affects and AQP4 recruitment may serve as reserve capacity for selective recruitment of glymphatic clearance, whether in response to increased demand by exercise or, potentially, in states of neurodegeneration. As such, further studies are needed to investigate the anatomic underpinnings and physiologic activity of this potential direct and recruitable CSF pathway as a possible biomarker for cognitive decline and/or therapeutic targeting. Due to the noninvasive and non-contrast methodology, it is possible to investigate intrinsic CSF outflow in early AD patients with active and sedentary lifestyles or effect of physical exercise.

Limitations

Our study enrolled a small number of participants, and used self-reported measures of physical activity and sedentary time to group individuals into active and sedentary groups. We asked sedentary individuals to increase their weekly activity levels recorded by fitbit or smart watch for 3 weeks and relied on self-report for compliance. Although results showed large differences between groups, and between pre- and post-exercise scans for the sedentary group, results must be replicated in a more rigorous study that obtains objective measures of activity levels. Furthermore, sleep is known to facilitate brain metabolite clearance in animals.[13] The prolonged sedentary behavior in humans may be associated with insomnia; therefore, poor quality of sleep may also influence the glymphatic clearance.[49] While we did not measure sleep, heart rate, or blood pressure, it is possible that the sedentary subjects may alter sleep quality after an exercise intervention.

Conclusion

In conclusion, our findings in healthy adults with active and sedentary lifestyles reveal differences in quantitative CSF outflow metrics related to activity levels. These quantitative outflow findings at the lower PSD add credence to the hypothesis

of a distinct, recruitable second pathway of CSF egress from the subpial space to the SSS, with potential implications for future use as a biomarker for cognitive decline and/or therapeutic targeting in aging and neurodegeneration.

Acknowledgments

We thank Professor Alexander Norbash, Department Chair of Radiology, University of California, San Diego for his support on this project, Ms. Diana Vucevic for fruitful discussion, and Dr. Xiaowei Zhang for his support on ROI segmentations. In addition, we thank Dr. Yoshimori Kassai and Mr. Yurian Falls of Canon Medical Systems for their technical support.

Funding

This work was supported by an NIH grant RF1AG076692 (Mitsue Miyazaki), and a grant by Canon Medical Systems, Japan (35938) (Mitsue Miyazaki). The funders had no role in study design, data collection, and interpretation, or the decision to submit the work for publication.

Conflicts of Interest

All authors have no conflicts of interest.

References

1. Patterson C. World Alzheimer Report 2018. The state of the art of dementia research: new frontiers. London:Alzheimer's Disease International, 2018.
2. Brookmeyer R, Abdalla N, Kawas CH, Corrada MM. Forecasting the prevalence of preclinical and clinical Alzheimer's disease in the United States. Alzheimers Dement 2018; 14:121–129.
3. Pike KE, Savage G, Villemagne VL, et al. Beta-amyloid imaging and memory in non-demented individuals: evidence for preclinical Alzheimer's disease. Brain 2007; 130:2837–2844.
4. Verheggen ICM, Van Boxtel MPJ, Verhey FRJ, Jansen JFA, Backes WH. Interaction between blood-brain barrier and glymphatic system in solute clearance. Neurosci Biobehav Rev 2018; 90:26–33.
5. Iliff JJ, Wang M, Liao Y, et al. A paravascular pathway facilitates CSF flow through the brain parenchyma and the clearance of interstitial solutes, including amyloid β. Sci Transl Med 2012; 4:147ra111.
6. Iliff JJ, Wang M, Zeppenfeld DM, et al. Cerebral arterial pulsation drives paravascular CSF-interstitial fluid exchange in the murine brain. J Neurosci 2013; 33:18190–18199.
7. Nedergaard M. Neuroscience. Garbage truck of the brain. Science 2013; 340:1529–1530.
8. Jessen NA, Munk AS, Lundgaard I, Nedergaard M. The glymphatic system: A beginner's guide. Neurochem Res 2015; 40:2583–2599.
9. Shibata M, Yamada S, Kumar SR, et al. Clearance of Alzheimer's amyloid-ss(1-40) peptide from brain by LDL receptor-related protein-1 at the blood-brain barrier. J Clin Invest 2000; 106:1489–1499.
10. Nedergaard M, Goldman SA. Glymphatic failure as a final common pathway to dementia. Science 2020; 370:50–56.
11. Benveniste H. The brain's waste-removal system. Cerebrum 2018; 2018:cer-09–cer-18.
12. Kress BT, Iliff JJ, Xia M, et al. Impairment of paravascular clearance pathways in the aging brain. Ann Neurol 2014; 76:845–861.
13. Xie L, Kang H, Xu Q, et al. Sleep drives metabolite clearance from the adult brain. Science 2013; 342:373–377.
14. He XF, Liu DX, Zhang Q, et al. Voluntary exercise promotes glymphatic clearance of amyloid beta and reduces the activation of astrocytes and microglia in aged mice. Front Mol Neurosci 2017; 10:144.
15. Absinta M, Ha SK, Nair G, et al. Human and nonhuman primate meninges harbor lymphatic vessels that can be visualized noninvasively by MRI. eLife 2017; 6:e29738.
16. Ringstad G, Eide PK. Cerebrospinal fluid tracer efflux to parasagittal dura in humans. Nat Commun 2020; 11:354.
17. Malis V, Bae WC, Yamamoto A, McEvoy LK, McDonald MA, Miyazaki M. Age-related decline of intrinsic cerebrospinal fluid outflow in healthy humans detected with non-contrast spin-labeling MR imaging. Online published. Magn Reson Med Sci 2022 December 17. [Epub ahead of print]
18. Pollay M. The function and structure of the cerebrospinal fluid outflow system. Cerebrospinal Fluid Res 2010; 7:9.
19. Sakka L, Coll G, Chazal J. Anatomy and physiology of cerebrospinal fluid. Eur Ann Otorhinolary 2011; 128:309–316.
20. Bull FC, Al-Ansari SS, Biddle S, et al. World Health Organization 2020 guidelines on physical activity and sedentary behaviour. Br J Sports Med 2020; 54:1451–1462.
21. von Holstein-Rathlou S, Petersen NC, Nedergaard M. Voluntary running enhances glymphatic influx in awake behaving, young mice. Neurosci Lett 2018; 662:253–258.
22. MacIntosh BJ, Crane DE, Sage MD, et al. Impact of a single bout of aerobic exercise on regional brain perfusion and activation responses in healthy young adults. PLoS One 2014; 9:e85163.
23. Ogawa T, Spina RJ, Martin WH 3rd, et al. Effects of aging, sex, and physical training on cardiovascular responses to exercise. Circulation 1992; 86:494–503.
24. Hamilton MT, Healy GN, Dunstan DW, Zderic TW, Owen N. Too little exercise and too much sitting: Inactivity physiology and the need for new recommendations on sedentary behavior. Curr Cardiovasc Risk Rep 2008; 2:292–298.
25. Ding D, Wang X, Li Q, Li L, Wu J. Research on the glial-lymphatic system and Its relationship with Alzheimer's disease. Front Neurosci 2021; 15:605586.
26. Craig CL, Marshall AL, Sjöström M, et al. International physical activity questionnaire: 12-country reliability and validity. Med Sci Sports Exerc 2003; 35:1381–1395.
27. Miyazaki M, Akahane M. Non-contrast enhanced MR angiography: established techniques. J Magn Reson Imaging 2012; 35:1–19.
28. Miyazaki M, Lee VS. Nonenhanced MR angiography. Radiology 2008; 248:20–43.
29. Miyazaki M, Isoda H. Non-contrast-enhanced MR angiography of abdomen. Eur J Radiol 2011; 80:9–23.

30. Miyazaki M, Zhou X, Hoshino T, Yokoyama K, Ishimura R, Nitatori T. Non-contrast myocardial perfusion using a novel 4D magnetic resonance arterial spin labeling technique: initial experience. Microvasc Res 2015; 98:94–101.
31. Huber F. A logical introduction to probability and induction. New York:Oxford University Press, 2018; p. 80.
32. Chan AA, Nelson SJ. Simplified gamma-variate fitting of perfusion curves. Proceedings of the 2nd IEEE International Symposium on Biomedical Imaging, Arlington, 2004; 1067–1070.
33. Hablitz LM, Pla V, Giannetto M, et al. Circadian control of brain glymphatic and lymphatic fluid flow. Nat Commun 2020; 11:4411.
34. Pollock H, Hutchings M, Weller RO, Zhang E-T. Perivascular spaces in the basal ganglia of the human brain: their relationship to lacunes. J Anat 1997; 191:337–346.
35. Wardlaw JM, Benveniste H, Nedergaard M, et al. Perivascular spaces in the brain: anatomy, physiology and pathology. Nat Rev Neurol 2020; 16:137–153.
36. Naganawa S, Ito R, Taoka T, Yoshida T, Sone M. The space between the pial sheath and the cortical venous wall may connect to the meningeal lymphatics. Magn Reson Med Sci 2020; 19:1–4.
37. Nakada T, Kwee IL, Igarashi H, Suzuki Y. Aquaporin-4 functionality and Virchow-Robin Space water dynamics: Physiological model for neurovascular coupling and glymphatic flow. Int J Mol Sci 2017; 18:1798.
38. Mestre H, Hablitz LM, Xavier AL, et al. Aquaporin-4-dependent glymphatic solute transport in the rodent brain. eLife 2018; 7:e40070.
39. Nagelhus EA, Ottersen OP. Physiological roles of aquaporin-4 in brain. Physiol Rev 2013; 93:1543–1562.
40. Day RE, Kitchen P, Owen DS, et al. Human aquaporins: regulators of transcellular water flow. Biochim Biophys Acta 2014; 1840:1492–1506.
41. Zeppenfeld DM, Simon M, Haswell JD, et al. Association of perivascular localization of Aquaporin-4 with cognition and Alzheimer disease in aging brains. JAMA Neurol 2017; 74:91–99.
42. Mader S, Brimberg L. Aquaporin-4 water channel in the brain and Its implication for health and disease. Cells 2019; 8:90.
43. Badaut J, Brunet JF, Grollimund L, et al. Aquaporin 1 and aquaporin 4 expression in human brain after subarachnoid hemorrhage and in peritumoral tissue. Acta Neurochir Suppl (Wien) 2003; 86:495–498.
44. Aoki K, Uchihara T, Tsuchiya K, Nakamura A, Ikeda K, Wakayama Y. Enhanced expression of aquaporin 4 in human brain with infarction. Acta Neuropathol 2003; 106:121–124.
45. Taoka T, Ito R, Nakamichi R, et al. Diffusion-weighted image analysis along the perivascular space (DWI-ALPS) for evaluating interstitial fluid status: age dependence in normal subjects. Jpn J Radiol 2022; 40:894–902.
46. Kamagata K, Andica C, Takabayashi K, et al. Association of MRI indices of glymphatic system with amyloid deposition and cognition in mild cognitive impairment and Alzheimer's disease. Neurology 2022; 99:e2648–e2660.
47. Pulous FE, Cruz-Hernández JC, Yang C, et al. Cerebrospinal fluid can exit into the skull bone marrow and instruct cranial hematopoiesis in mice with bacterial meningitis. Nat Neurosci 2022; 25:567–576.
48. Ahn JH, Cho H, Kim JH, et al. Meningeal lymphatic vessels at the skull base drain cerebrospinal fluid. Nature 2019; 572:62–66.
49. Yang Y, Shin JC, Li D, An R. Sedentary behavior and sleep problems: a systematic review and meta-analysis. Int J Behav Med 2017; 24:481–492.